Syddansk Universitet

Spin–orbit coupling in actinide cations

Bagus, Paul S.; Ilton, Eugene S.; Martin, Richard L.; Jensen, Hans Jørgen Aagaard; Knecht,
Stefan

Spin–orbit coupling in actinide cations

Paul S. Bagus [a,*], Eugene S. Ilton [b], Richard L. Martin [c], Hans Jørgen Aa. Jensen [d], Stefan Knecht [d]

[a] Department of Chemistry, University of North Texas, Denton, TX 76203-5017, USA
[b] Pacific Northwest National Laboratory, Richland, WA 99352, USA
[c] Theoretical Division MSB268, Los Alamos National Laboratory, Los Alamos, NM 87545, USA
[d] Department of Physics, Chemistry, and Pharmacy, University of Southern Denmark, DK-5230 Odense M, Denmark

ABSTRACT

The limiting case of Russell–Saunders coupling, which leads to a maximum spin alignment for the open shell electrons, usually explains the properties of high spin ionic crystals with transition metals. For actinide compounds, the spin–orbit splitting is large enough to cause a significantly reduced spin alignment. Novel concepts are used to explain the dependence of the spin alignment on the 5f shell occupation. We present evidence that the XPS of ionic actinide materials may provide direct information about the angular momentum coupling within the 5f shell.

© 2012 Elsevier B.V. All rights reserved.

1. Introduction

The analysis of the properties of high spin ionic transition metal crystals is based largely on the use of crystal and ligand field theory [1,2]. In this approach, the metal cation is in its Hund's rule ground state multiplet where the spins of the open d shell have the maximum possible spin alignment, or spin multiplicity, and the orbital angular momentum takes the maximum possible value consistent with this multiplicity. When crystal field effects are taken into account, the spatial symmetry is lowered but the spin alignment remains. The covalent mixing of cation and ligand orbitals is an additional perturbation to the free ion description introduced in ligand field theory; see Ref. [3] for a modern analysis of this covalent mixing. These theoretical approaches have been quite successful to predict and explain the physical and chemical properties of transition metal oxides, especially those of the 3d transition metal series. The concept of maximum spin alignment has also been used in studies of the electronic structure and magnetic properties of heavy metal oxides, especially actinide oxides; see, for example Refs. [4,5]. Thus, for example, each U^{4+} cation in UO_2 is assumed, in band structure calculations [5,6], to have 2 spins aligned parallel for a total $S_z = 1$. Of course, since UO_2 is an anti-ferromagnet, the spins on each cation would be aligned anti-parallel to those on neighboring cations. However, for heavy metals, spin–orbit splitting may significantly modify this analysis. This modification, and the resulting changes in the effective magnetic moment per cation, μ, were recognized in early crystal field, CF, studies of ionic actinide systems; see, for example, Ref. [7] where CF and spin–orbit splittings were combined to determine the effective magnetic moment of UO_2. However, CF calculations depend strongly on the choices made

for several parameters. Quite recently, a DFT + U calculation for UO_2 [6] has been used to parameterize a model Hamiltonian CF treatment that includes spin–orbit splitting. Unfortunately, DFT + U calculations [6], as with the earlier CF work [7], depend on choices of parameters. In this Letter, we report a systematic analysis of the effect of spin–orbit splitting on the spin alignment of actinide cations. Our results have a direct importance for the magnetic properties of actinide compounds and may provide information about the limitations of assumptions of maximum alignment in heavy metal oxides. Our predictions might, as we indicate below, be examined with XPS studies. We use a novel analysis based on the expectation values of quantum mechanical operators. These are $\langle L_z \rangle$ and $\langle S_z \rangle$ for the orbital and spin angular momenta, respectively, and the second quantization number operators [8] for the $5f_{5/2}$ and $5f_{7/2}$ occupations, denoted $N(5f_{5/2})$ and $N(5f_{7/2})$. To the best of our knowledge, these expectation values have never been used before to characterize the extent of intermediate coupling. We have also applied a technique we developed earlier [9], to determine the contributions of different Russell–Saunders, RS, multiplets to the relativistic J levels. These methods of analysis allow a transparent understanding of the intermediate coupling between RS multiplets and the relativistic limit of j–j coupling [10]. Our approach is in strong contrast to earlier treatments of the spin–orbit splitting and the angular momentum coupling in actinide metals [11–13], which were based on mathematical analyses of the angular momentum coupling as given by suitable Clebsch-Gordon coefficients.

2. Theoretical methods and computational details

We have computed wavefunctions, WF's, for low-lying electronic states of $5f^n$ open shell configurations of U, Pu, and Am cations. Four component Dirac-Hartree–Fock spinors were

* Corresponding author. Fax: +1 512 502 9760.
E-mail address: bagus@unt.edu (P.S. Bagus).

determined for the average of configurations of the $5f^n$ occupations.[14,15] The spinors were constrained to be eigenfunctions of j_z with quantum numbers m_j. These spinors were then used to determine complete open shell configuration interaction, COSCI, wavefunctions where all possible determinants with n electrons distributed over the 14 5f spinors were mixed. [15] The mixings were constrained so that all determinants mixed had the same total value of M_J. These WF's are eigenfunctions of J^2 and J_z; they include all the different levels that can be formed from the $5f^n$ configuration and allow intermediate angular momentum coupling. We are able to determine the energetic ordering of the levels, both for a given value of J and between different J values. For the $5f^n$ configurations non-relativistic WF's were calculated by using a value for the speed of light of $c = 15\,000$ a.u., which is two orders of magnitude larger than the correct value of $c = 137$ a.u. In the limit of $c \rightarrow \infty$, the exact solutions of the Dirac–Fock equations reduce to the non-relativistic solutions where the radial parts of the $\ell + 1/2$ and $\ell - 1/2$ are identical. We have confirmed that $c = 15,000$ provides a sufficiently accurate approximation to the non-relativistic limit; for example, the energies of the levels have the degeneracy for RS coupling to within a few micro-eV. In the non-relativistic limit, the COSCI solutions correspond to WF's for different states of the RS ^{2S+1}L multiplets. The uncontracted large component basis sets were taken from the basis sets optimized by Dyall [16] for the neutral atoms and are available from the Dirac web site, http://dirac.chem.vu.nl. The basis sets for the small components were generated from the large component sets by restricted kinetic balance [15,17]. The calculations of the spinors and the COSCI WF's were performed using the DIRAC program system [18].

3. Results and discussion

We begin with a brief review contrasting the limiting cases of angular momentum coupling. With Russell–Saunders or L–S coupling, the open atomic sub-shell $n\ell$ with n electrons, $(n\ell)^n$, couples to multiplets ^{2S+1}L where Hund's rules give the lowest energy multiplet. Neglecting spin–orbit splitting we focus on the state of this lowest energy multiplet with $M_L = \langle L_z \rangle = L$ and $M_S = \langle S_z \rangle = S$ since all states can be rotated into this state by a suitable coordinate transformation. Thus, each cation has maximum spin alignment. Once, spin–orbit splitting is taken into account and L and S couple to a J value, M_L and M_S are not, in general, good quantum numbers although there will always be a state for the maximum $J = L + S$, where M_J, M_L, and M_S are good quantum numbers. At the extreme where spin–orbit splittings are large, j–j coupling is appropriate and we first fill the $j = \ell - 1/2$ sub-shell and then fill the $j = \ell + 1/2$ sub-shell. Here, we obtain relativistic WF's and properties for intermediate coupling. For these WF's, we analyze the $\langle L_z \rangle$ and $\langle S_z \rangle$ and the occupations, $N(5f_{5/2})$ and $N(5f_{7/2})$. With the multiplet WF's from the non-relativistic calculations, we determine the contributions of RS multiplets to the different J levels [9].

In order to illustrate our methods of analysis, we compare, in Table 1, our results for $V^{2+}(3d^2)$ and $U^{4+}(5f^2)$. Both of these cations have triplet lowest RS multiplets with total spin of 1; however, the spin–orbit splittings lead to very different relative energies for the J levels that can arise from the RS multiplets for the light V and the heavy U cations. In the table, we give the energies of the suitable J levels, relative to the lowest level at $\Delta E = 0$ and the percent character of the RS lowest multiplet, ^3F and ^3H for V^{3+} and U^{4+} respectively, in these levels. We also give the $\langle S_z \rangle$, $\langle L_z \rangle$, and the occupation numbers, N, for the spin–orbit split $j = \ell + 1/2$ and $j = \ell - 1/2$ spinors; for the $\langle S_z \rangle$ and $\langle L_z \rangle$, we choose the state with $M_J = J$ as the definition of the z axis. For U, we give the intermediate coupling relativistic results and the non-relativistic limits where the J levels are rotations of the RS multiplet states; of course in

Table 1
Properties of the lowest levels of V^{3+} and U^{4+} for suitable J values, see text. The properties are for relativistic WF's that include intermediate coupling; for U, non-relativistic limits are also given. We give: the energy of the levels relative to the lowest energy level, ΔE; the percent of character that arises from the ^3F or ^3H RS multiplets; and the expectation values of S_z, L_z, and the $5f_j$ number operators. The $\langle S_z \rangle$ and $\langle L_z \rangle$ are given for the state with $M_J = J$, all other properties are the same for all states in the level.

$V^{3+}(3d^2)$					
J	ΔE(eV)	%(^3F)	$\langle S_z \rangle$	$\langle L_z \rangle$	$N(3d_{3/2})$	$N(3d_{5/2})$
Relativistic intermediate coupling						
2	0.00	99.94	−0.67	+2.67	1.63	0.37
3	0.04	100	+0.25	+2.75	1.00	1.00
4	0.10	99.99	+1.00	+3.00	0.21	1.79

$U^{4+}(5f^2)$					
J	ΔE(eV)	%(^3H)	$\langle S_z \rangle$	$\langle L_z \rangle$	$N(5f_{5/2})$	$N(5f_{7/2})$
Relativistic intermediate coupling						
4	0.00	91	−0.72	+4.72	1.95	0.05
5	0.73	100	+0.17	+4.83	1.00	1.00
6	1.41	98	+0.98	+5.02	0.26	1.74
Non-relativistic limits						
4	0.00	100	−0.80	+4.80	1.71	0.29
5	0.00	100	+0.17	+4.83	1.00	1.00
6	0.00	100	+1.00	+5.00	0.15	1.85

the non-relativistic limit, the energies of the different J levels for a given RS multiplet are the same. For V, we give only the intermediate coupling results since departures from RS coupling are negligible.

The $J = 2$, 3, and 4 are the lowest levels for the d^2 configuration of V^{3+}. The highest $J = 4$ level is only 0.1 eV above the lowest $J = 2$ level; the calculated ΔE are very close to the experimental values for V^{+3} energies [19]. From the projections of the RS ^3F multiplet on the J levels, it is clear that the contributions of other multiplets are negligible and V can be accurately described at the RS limit. The energetic ordering of the levels is consistent with the occupations of the spin–orbit split 3d orbitals; $J = 2$ has the smallest occupation of the higher orbitals, $N(3d_{5/2})$, while $J = 4$ has the largest value of $N(3d_{5/2})$. While the highest $J = 4$ level has the expected $\langle S_z \rangle = 1$ corresponding to two spins aligned parallel, the $\langle S_z \rangle$ for the lower lying $J = 2$, and $J = 3$ levels are significantly reduced in magnitude from 1. The origin of this reduction is simply the change from the representation where L, S, M_L, and M_S are good quantum numbers to one where J, L, S, and M_J are good quantum numbers [10]. However, the excitation energy to the $J = 4$ level is sufficiently small that the coupling of S and L on neighboring metal cations in high spin V_2O_3, as given for example by a Heisenberg Hamiltonian, [20] would be sufficient to offset the small spin–orbit coupling that makes $J = 2$ the lowest level with the concomitant reduction is spin alignment.

As shown in Table 1, while there are similarities between the properties of the $5f^2$ configuration of U^{4+} with those of the $3d^2$ configuration of V^{3+}, there are also significant differences because the spin–orbit coupling is much larger for U than for V. Before we discuss these differences, we note that the excitation energies, ΔE's, presented in Table 1 are remarkably similar to the experimental values for the gas phase U^{4+} cation [21]. Our errors for the ΔE's are ≤0.03 eV for ΔE that are ~1 eV. The agreement with experiment that we have found for both V^{3+} and U^{4+} provide evidence that our COSCI wavefunctions are adequate to allow us to interpret the intermediate coupling for U^{4+} and the other actinide cations that we discuss later. Having established the quality of our theoretical model, we turn to an analysis of the Hund's rules ^3H RS multiplet for $U^{4+}(5f^2)$, which has $J = 4$, 5, and 6 levels. The lowest level for U^{4+} is $J = 4$ that is dominated by the ^3H multiplet with a 91% contribution and with 1% and 9% contributions from $^3F_4$ and $^1G_4$, respectively. The lowest level with $J = 5$ is at $\Delta E = 0.73$ eV and is

100% ^3H; the lowest level with $J = 6$ is at $\Delta E = 1.4$ eV and is 98% ^3H. While the $J = 5$ level that is $^3H_5$ is the second level of U^{4+}, the excited $J = 6$ level that is dominated by the ^3H multiplet is so high in energy that there are three intervening levels, with $J = 2, 4,$ and 3. As for V^{3+}, the energetic ordering of the U^{4+} levels is consistent with the occupations of the $5f_{5/2}$ and $5f_{7/2}$ spinors where the lowest $J = 4$ level has $N(5f_{5/2})$ almost 2. As for the case of V^{3+}, the highest level has the spin alignment expected for the ^3H multiplet with $\langle S_z \rangle = 0.98$; the small departure from the value of $\langle S_z \rangle = 1.00$ for $^3H_6$ is because there is a small, 2%, contribution of the ^1I RS multiplet to this $J = 6$ level. The $J = 4$ level has a magnitude of $\langle S_z \rangle$ smaller by more than 25% from the value expected for two aligned spins. Furthermore, the excited levels of U^{4+} are sufficiently high in ΔE that the properties of a U^{4+} cation in the crystal field of UO_2 will be dominated by the lowest $J = 4$ level with the reduced spin alignment. In this context, we note that the excitation energy to the $J = 6$ level is almost 3 orders of magnitude larger than kT at the UO_2 Neel temperature [22] of 31 K. The main reason for the changes in the spin alignment is the re-coupling of the RS states to form eigenfunctions of J^2 rather than to relativistic changes in the spinors. The properties of the non-relativistic limits of the pure ^3H_J levels, shown in Table 1, are similar to the relativistic values with the differences arising from the mixing, as discussed above, of other RS multiplets in the $J = 4$ and $J = 6$ levels. The comparison of the spin–orbit splitting of the levels in V^{3+} with those in U^{4+} showed how important relativistic effects are to determine the energy spacing of different J levels, For heavy metals the lowest J level, which has a different spin-alignment than expected from RS coupling, must be used. However, as we show in Table 1, the changes in the spin alignment of the lowest J level arise mainly because of the angular momentum coupling to form eigenfunctions of J^2 and not because the $j = \ell - \frac{1}{2}$ and $j = \ell + \frac{1}{2}$ spinors have a different radial function.

We now consider an embedded UO_8 cluster model of bulk UO_2 in order to show that the results that we have presented above are relevant for condensed systems; the UO_8 cluster model and WF's are given in Ref. [23]. The ligand field splits the six $5f_{5/2}$ and eight $5f_{7/2}$ atomic spinors into molecular levels for the O_h double group, the doubly degenerate γ_{6u} and γ_{7u} and the fourfold degenerate γ_{8u}. Rather than distinguishing the γ_{6u} and γ_{7u} representations, we use the more familiar notations a and e to separate the doubly and four fold degenerate representations. The cluster spinors also have a small amount of covalent anti-bonding character with O spinors, which is measured by projecting the $5f_j$ spinors of the isolated U^{4+} cation on the spinors for UO_2. [24] The cluster model spinors are denoted by '5/2' and '7/2' to indicate this covalent character. The ligand field splittings of the spinor orbital energies and the atomic projections are given in Table 2. The 0.8 eV spin–orbit splitting of the atomic $5f_{5/2}$ and $5f_{7/2}$ orbital energies is perturbed by the ligand field and there is a small mixing of $f_{5/2}$ and $f_{7/2}$ character in one pair of '5/2' and '7/2' orbitals. The cluster spinors are dominantly on U and the covalent U(5f)-O mixing has a maximum of 7% for the higher energy '7/2' a orbital. The 9 degenerate states of the lowest U^{4+} $J = 4$ level are split in the lower O_h double group

Table 3
Intermediate coupling results for levels of different charge states of the Am cation. The levels are characterized by the expectation values of S and L and by the occupations of the spin–orbit split $5f_j$ sub-shells. The Hund's rule RS multiplet and the per cent character of this multiplet projected from the intermediate coupling levels are also given.

J	ΔE(eV)	$\langle S_z \rangle$	$\langle L_z \rangle$	$N(5f_{5/2})$	$N(5f_{7/2})$	% Hund's multiplet
Am(4+;5f^5) – Hund's rule ^6H						
5/2	0.00	−1.57	+4.07	4.03	0.97	76
7/2	0.46	−0.52	+4.02	3.45	1.55	86
15/2	1.94	+1.91	+5.59	2.77	2.23	62
Am(3+;5f^6) – Hund's rule ^7F						
0	0.00	+0.00	+0.00	4.76	1.24	63
1	0.24	+0.50	+0.50	4.21	1.80	76
6	1.48	+2.76	+3.24	3.12	2.88	79
Am(2+;5f^7) – Hund's rule ^8S						
7/2	0.00	+3.36	+0.12	3.73	3.27	89
7/2	2.86	+1.89	+1.61	4.57	2.43	7

symmetry over an energy range of 0.20 eV. Further, the occupations of the '5/2' and '7/2' spinors for the lowest energy states of UO_2 are almost the same, dominantly $5f_{5/2}$ with $N('5/2') = 1.93$ and $N('7/2') = 0.07$, as for the isolated cation. Clearly, the atomic character of the open shell 5f spinors for U^{4+} persists in UO_2 and we expect that the spin alignment character also deviates from the nominal $\langle S_z \rangle = 1.00$ for condensed ionic UO_2, as for the U^{4+} cation. Our conclusion from the cluster comparisons that UO_2 is well in the ionic, free ion, limit is consistent with earlier periodic hybrid DFT calculations, [25] recent angle-resolved photoemission, [26] and X-ray absorption studies. [27,28].

We now turn to a later member of the actinide series, Americium. Intermediate coupling results for three different charge states of the Am cations, $Am^{4+}(5f^5)$, $Am^{3+}(5f^6)$, and $Am^{2+}(5f^7)$, are given in Table 3 where the coupling is characterized, as in Table 1, with $\langle S_z \rangle$, $\langle L_z \rangle$, $N(5f_{5/2})$, and $N(5f_{7/2})$. The Hund's rules ground state multiplets and the projection of these multiplets on the relativistic levels are also given in Table 3. With this series, our goal is to examine the influence of approaching half-filling of the f-shell on the intermediate coupling. The two lowest levels are shown for each charge state; for the first two $5f^n$ configurations, we also give the first excited level with the maximum J value for the Hund's rules lowest RS multiplet since this is the level that could have the $\langle S_z \rangle$ expected for maximum spin alignment. For the $5f^7$ half-filled shell, the two lowest levels are both $J = 7/2$ and this corresponds to the situation where maximum spin alignment is possible. For the lowest $5f^7$ level, $\langle S_z \rangle = 3.36$ and $\langle L_z \rangle = 0.12$ are close to the values of 3.5 and 0.0 for a pure RS ^8S multiplet. For this level, there is also a large occupation of the excited $5f_{7/2}$ shell, $N(5f_{7/2}) = 3.27$. For the non-relativistic limit of the ^8S RS multiplet, the occupations are $N(5f_{5/2}) = 3$ and $N(5f_{5/2}) = 4$. While intermediate coupling for this level has a higher $N(5f_{5/2})$ than the non-relativistic ^8S limit, there is a considerable energetic cost in promoting over two electrons from $5f_{5/2}$ to $5f_{7/2}$. The approximation of maximum spin alignment is reasonable for the $5f^7$ configuration since the high spin coupling is favored by 21 5f–5f exchange interactions, sufficient to largely overcome the spin–orbit penalty for a large occupation of the $5f_{7/2}$ sub-shell. This is also reflected in the fact that the first excited state, where the occupation of the $5f_{5/2}$ sub-shell is larger, lies at much higher energy, $\Delta E = 2.9$ eV.

The results are quite different for the other $5f^n$ occupations. For $5f^6$, the lowest level is $J = 0$ with no magnetic properties since $\langle S_z \rangle = \langle L_z \rangle = 0$. This result might be expected from the fact the $5f^6$ will just fill the lower $5f_{5/2}$ shell. It is not quite this simple since the occupations of the f sub-shells are $N(5f_{5/2}) \sim 5$ and $N(5f_{7/2}) \sim 1$. It is interesting that the first excited level is very low-lying at $\Delta E = 0.24$ eV and corresponds roughly to promotion of an electron

Table 2
Orbital energies, point group symmetry, and atomic projections of the open shell orbitals of the UO_8 cluster model of UO_2; see text.

UO_8 open shells			Atomic projection	
Type	Sym	ΔE (eV)	$5f_{5/2}$	$5f_{7/2}$
'5/2'	e	0	0.97	0.00
'5/2'	a	0.17	0.85	0.12
'7/2'	a	0.62	0.00	0.97
'7/2'	e	0.67	0.00	0.97
'7/2'	a	1.31	0.10	0.83

from $5f_{5/2}$ to $5f_{7/2}$. However, $\langle S_z \rangle = 0.5$ is less than 20% of the $\langle S_z \rangle = 3.0$ expected for the ^7F Hund's rules lowest RS multiplet. The lowest $J = 6$ level is at $\Delta E = 1.5$ eV and approaches the properties and spin alignment expected for a ^7F multiplet. For $5f^5$, all the levels shown have substantial departures from the $\langle S_z \rangle = 2.5$ expected for the lowest RS ^6H multiplet. Even for the $J = 15/2$ level at $\Delta E = 1.9$ eV that could give the ^6H spin alignment, $\langle S_z \rangle$ is less than 20% of the nominal value. Results, not shown, for other actinide cations, in particular Cm, and Pu, have similar departures from the ideal spin alignment expected from Hund's rule. The projections of the Hund's rules ground state multiplet on the relativistic levels, where intermediate coupling is included, also show that the departures from RS coupling for the $5f^5$ and $5f^6$ configurations are very large. On the other hand, for $5f^7$, the projection of the ^8S multiplet on the lowest $J = 0$ level does show that this multiplet makes the dominant contribution. All our evidence shows that, except for the $5f^7$ half-filled shell, there is considerable deviation from the spin alignment expected from Hund's rules multiplets. From the occupation numbers, it is also clear that the states are not well described in the pure j-j coupling limit either.

The intermediate coupling of the open f shell also contributes to the X-ray photoemission spectra, XPS, of these actinide cations. In order to show the importance of intermediate coupling for the XPS,

we contrast the 4f XPS for the $J = 7/2$ ground state of $Am^{2+}(5f^7)$ and the $J = 0$ ground state of $Am^{3+}(5f^6)$ cations since these represent cases near the limits of RS coupling for Am^{2+} and j–j coupling for Am^{3+}. Similar procedures as for the ground states were used to determine the 4f-hole state WF's. The Dirac Hartree–Fock spinors were computed for the averages of the $4f^{13}5f^n$ configurations and COSCI WF's were calculated for the distributions of the 4f hole over all possible 4f spinors together with the distributions of the n 5f electrons over all possible 5f spinors. This constraint for the distribution of electrons between the open core and the open valence shells accounts for the angular momentum coupling and re-coupling needed to correctly describe core-level XPS spectra. [3,29] The relative intensities, I_{rel}, of the XPS peaks are determined using the Sudden Approximation, SA [3,30] which is correct in the limit of high photon energy. However, the SA I_{rel} are reasonably accurate at photon energies a few 100's of eV above threshold; see, for example, Ref. [31]. The programs for the calculation of the SA I_{rel} have been adapted from programs in the CLIPS package. [32] Our approach here follows the same procedures as used in our earlier work on the 4f XPS of U^{4+} and U^{5+} cations. [23,33,34] In Figure 1a and b, we give our theoretical 4f XPS for Am^{2+} and Am^{3+}. The contributions of the individual 4f-hole states have been broadened by Gaussians with a 0.75 eV full width at half-maximum, FWHM, to
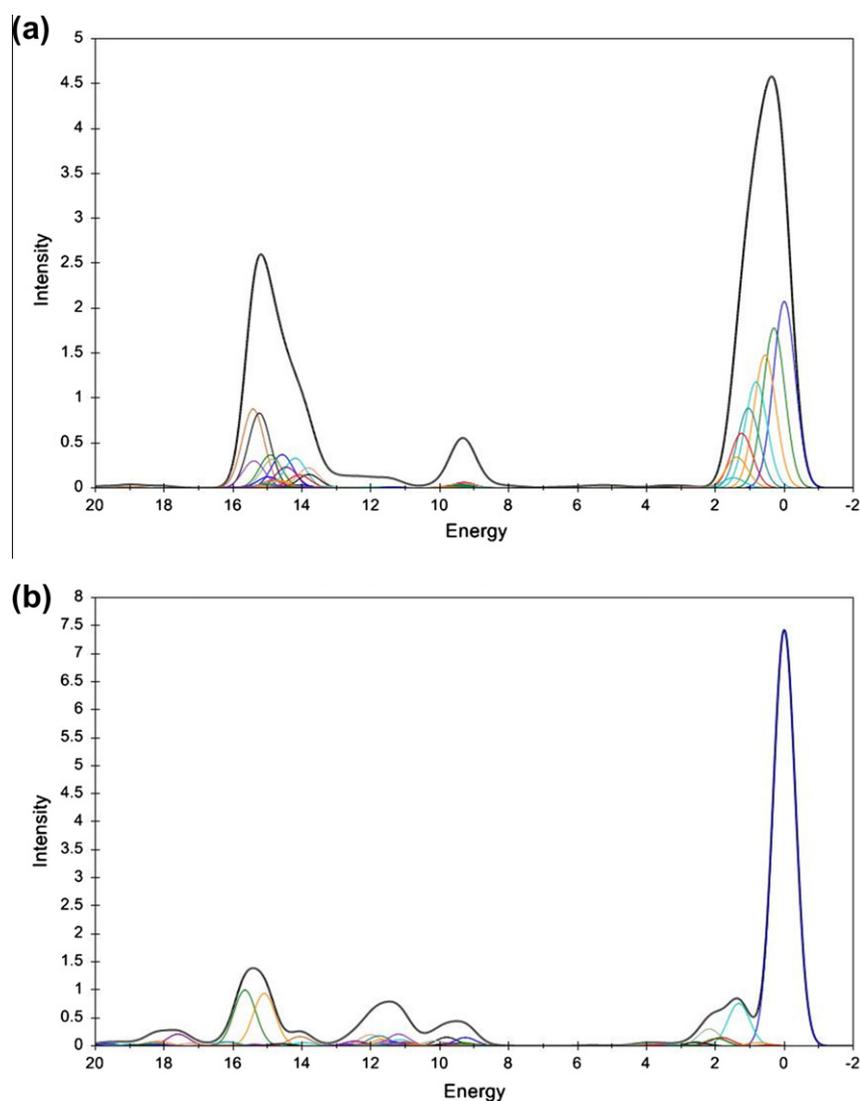

Figure 1. Predicted 4f XPS for a) $Am^{2+}(5f^7)$ and b) $Am^{3+}(5f^6)$.

take into account the instrumental and intrinsic broadening of the XPS peaks that is present in all measured XPS spectra. The dark curves in the figure are the sum of all individual contributions, while the individual contributions with the largest intensities are shown as lighter curves.

For the $5f^7$ configuration of Am^{2+}, the FWHM of the leading, $4f_{7/2}$ XPS peak, ~1.5 eV, is twice as large as the broadening of the individual states and is skewed to higher BE,. The large increase in broadening is due to the angular momentum coupling of the $4f_{7/2}$ core–hole and the $J = 7/2$ coupling of the $5f^7$ open shell leading to final state multiplets of $J = 7, 6, 5, 4, 3, 2, 1,$ and 0. The $J = 7$ 4f-hole level has the lowest energy and the lower J levels have progressively higher energies; the separations between these individual levels, especially for the higher J levels that have higher intensity, are between 0.25 and 0.3 eV. The unresolved superposition of these peaks leads to a broad peak with a FWHM that is twice as large as the FWHM used for the individual peaks. Unresolved multiplet splittings also lead to a broad initial peak in the 2p XPS of MnO [29] because of the coupling of the open $2p_{3/2}$ shell with the half filled $3d^5$ shell that is coupled to a ^6S RS multiplet. The energy separations of the multiplets in the 2p XPS of Mn^{2+} are considerably larger than for the 4f XPS of Am^{2+} because the 2p–3d exchange integrals in 3d transition metals are much larger than the 4f–5f exchange integrals in actinides [23]. However, the physical reason for the broadening of the peaks for Am^{2+} and Mn^{2+} is the same, the multiplet splitting of a core hole with a high spin coupled valence open shell. The situation is quite different for the $4f^6$ configuration of Am^{3+}. Here, the leading $4f_{7/2}$ XPS peak is dominantly from a single state with a FWHM that is the assumed broadening; there are shake satellites between ~1.3 and ~2.6 eV that have 20% of the intensity of the single main peak. This leading edge is clearly different from the XPS for $5f^7$. There are also major differences of the dominantly $4f_{5/2}$ XPS at ~15 eV relative to the main peak. These structures arise from angular momentum coupling for the $5f^7$ case and from shake within the 5f shell for both $5f^7$ and $5f^6$. Clearly, the different angular momentum coupling of the electrons in the 5f shell in these two cases must be taken into account for a correct interpretation of the XPS spectra. While the spectra that we have shown are for isolated cations and do not include molecular, or extra-atomic, many body effects, the spectra for metal oxides also reflect atomic as well as molecular many body-effects. The different atomic many-body effects for the XPS that arise from the intermediate angular momentum coupling within the 5f shell must be taken into account in order to have a correct interpretation.

4. Conclusions

In summary, we have used novel criteria of the expectation values of the spin and orbital angular momentum, of the $5f_j$ number operators, and of the projection of RS multiplets on J levels to demonstrate and quantify the importance of intermediate coupling for actinide cations. These criteria show that, as a consequence of the relatively large spin–orbit splitting, the lowest J levels of an actinide cation have much higher $5f_{5/2}$ occupation, $N(5f_{5/2})$, than $5f_{7/2}$ occupation, $N(5f_{7/2})$. This, in turn, leads to a lowering of the spin alignment from that expected using RS multiplets and neglecting spin–orbit splitting. Furthermore, the energy lowering of the levels with large $N(5f_{5/2})$ is large, especially compared with the energies associated with anti-ferromagnetic ordering. Thus, even when the Hund's rules RS multiplet dominates for a given J level, there are significant deviations from the maximum spin alignment expected from a non-relativistic analysis. An exception is the half filled, $5f^7$, shell where the large number of exchange interactions favor maximum spin alignment; this is consistent

with earlier studies of Cm metal [13]. The reductions that we predict for the average spin alignment should lead to relatively low Neel temperatures for anti-ferromagnetic actinide oxides. Indeed, a relatively small Neel temperature of 31 K [22] is found for UO_2 as compared to 116 K for MnO [35]. However, the reduced metal–ligand overlap in the actinide series could also contribute to smaller anti-ferromagnetic coupling as well. We have also shown that the character of the angular momentum coupling in the open 5f shell has a strong influence on the character of XPS spectra of actinide cations. It would be valuable if XPS experiments for the different coupling of the $5f^6$ and $5f^7$ occupations of ionic actinide materials would confirm the predictions that we have presented.

References

[1] J.S. Griffith, The Theory of Transition-Metal Ions, Cambridge Press, Cambridge, 1971.
[2] L.E. Orgel, An Introduction to Transition-Metal Chemistry, John Wiley & Sons, New York, 1966.
[3] P.S. Bagus, E.S. Ilton, Phys. Rev. B 73 (2006) 155110.
[4] L.P. Spencer et al., Angew. Chem., Int. Ed. 48 (2009) 3795.
[5] I.D. Prodan, G.E. Scuseria, R.L. Martin, Phys. Rev. B 76 (2007) 033101.
[6] F. Zhou, V. Ozolins, Phys. Rev. B 83 (2011) 085106.
[7] H.U. Rahman, W.A. Runciman, J. Phys. Chem. Solids 27 (1966) 1833.
[8] L.D. Landau, E. M. Lifshitz, Quantum Mechanics, Addison-Wesley, Reading, 1958.
[9] P.S. Bagus et al., Chem. Phys. Lett. 455 (2008) 331.
[10] E.U. Condon, G.H. Shortly, The Theory of Atomic Spectra, Cambridge University Press, Cambridge, 1951.
[11] K.T. Moore et al., Phys. Rev. Lett. 90 (2003) 196404.
[12] G. van der Laan et al., Phys. Rev. Lett. 93 (2004) 097401.
[13] K.T. Moore et al., Phys. Rev. Lett. 98 (2007) 236462.
[14] J. Thyssen, Ph.D. dissertation, University of Southern Denmark, 2001.
[15] L. Visscher et al., Comput. Phys. Commun. 81 (1994) 120.
[16] K.G. Dyall, Theor. Chem. Acc. 117 (2007) 491.
[17] K.G. Dyall, K. Faegri Jr., Introduction to Relativistic Quantum Chemistry, New York, Oxford, 2007.
[18] DIRAC, a relativistic ab initio electronic structure program, Release DIRAC08 (2008), written by L. Visscher, H. J. Aa. Jensen, and T. Saue, with new contributions from R. Bast, S. Dubillard, K. G. Dyall, U. Ekström, E. Eliav, T. Fleig, A. S. P. Gomes, T. U. Helgaker, J. Henriksson, M. Iliaš, Ch. R. Jacob, S. Knecht, P. Norman, J. Olsen, M. Pernpointner, K. Ruud, P. Sałek, J. Sikkema (see the URL at <http://dirac.chem.sdu.dk>).
[19] C.E. Moore, Atomic Energy Levels, Natl. Bur. Stand. No. 467, US GPO, Washington, DC 1952, see also, URL <http://physics.nist.gov/cgi-bin/AtData/main_asd>.
[20] N. W. Ashcroft, N. D. Mermin, Solid State Physics, Holt, Rinehart, and Winston, NY, 1976.
[21] J.F. Wyart, V. Kaufman, J. Sugar, Phys. Scr. 22 (1980) 389.
[22] B.C. Frazer et al., Phys. Rev. 140 (1965) A1448.
[23] E.S. Ilton, P.S. Bagus, Surf. Sci. 602 (2008) 1114.
[24] C.J. Nelin, P.S. Bagus, M.R. Philpott, J. Chem. Phys. 87 (1987) 2170.
[25] K.N. Kudin, G.E. Scuseria, R.L. Martin, Phys. Rev. Lett. 89 (2002) 266402.
[26] L.E. Roy et al., J. Comput. Chem. 29 (2008) 2288.
[27] J.G. Tobin, S.W. Yu, Phys. Rev. Lett. 107 (2011) 167406.
[28] S.W. Yu et al., Phys. Rev. B 83 (2011) 165102.
[29] P.S. Bagus et al., Phys. Rev. Lett. 84 (2000) 2259.
[30] T. Aberg, Phys. Rev. 156 (1967) 35.
[31] B.D. Hermsmeier et al., Phys. Rev. B 48 (1993) 12425.
[32] CLIPS, is a program system to compute ab initio SCF and correlated wavefunctions for polyatomic systems. It has been developed based on the publicly available programs in the ALCHEMY package from the IBM San Jose Research Laboratory by P. S. Bagus, B. Liu, A. D. McLean, and M. Yoshimine.
[33] P.S. Bagus, E.S. Ilton, Theor. Chem. Acc. 118 (2007) 495.
[34] E.S. Ilton, P.S. Bagus, Phys. Rev. B 71 (2005) 195121.
[35] C. Kittel, Introduction to Solid State Physics, John Wiley & Sons, New York, 1976.